



# Hydrogeochemical characteristics and recharge sources identification based on isotopic tracing of alpine rivers in the Tibetan Plateau

Ruiyin Han<sup>a,b</sup>, Wenjing Liu<sup>a,b,c</sup>, Jiangyi Zhang<sup>a,b,c</sup>, Tong Zhao<sup>a,b,c</sup>, Huiguo Sun<sup>a,b,c</sup>, Zhifang Xu<sup>a,b,c,\*</sup>

<sup>a</sup> Key Laboratory of Cenozoic Geology and Environment, Institute of Geology and Geophysics, Chinese Academy of Sciences, Beijing, 100029, China

<sup>b</sup> University of Chinese Academy of Sciences, Beijing, 100049, China

<sup>c</sup> CAS Center for Excellence in Life and Paleoenvironment, Beijing, 100044, China

## ARTICLE INFO

Handling Editor: Robert Letcher

**Keywords:**

Tibetan Plateau  
Alpine river  
Hydrochemistry  
Major ions  
Isotopic tracing

## ABSTRACT

Alpine rivers originating from the Tibetan Plateau (TP) contain large amounts of water resources with high environmental sensitivity and eco-fragility. To clarify the variability and controlling factors of hydrochemistry on the headwater of the Yarlung Tsangpo River (YTR), the large river basin with the highest altitude in the world, water samples from the Chaiqu watershed were collected in 2018, and major ions,  $\delta^2\text{H}$  and  $\delta^{18}\text{O}$  of river water were analyzed. The values of  $\delta^2\text{H}$  (mean:  $-141.4\text{\textperthousand}$ ) and  $\delta^{18}\text{O}$  (mean:  $-18.6\text{\textperthousand}$ ) were lower than those in most Tibetan rivers, which followed the relationship:  $\delta^2\text{H} = 4.79 * \delta^{18}\text{O} - 52.2$ . Most river deuterium excess (d-excess) values were lower than 10‰ and positively correlated with altitude controlled by regional evaporation. The  $\text{SO}_4^{2-}$  in the upstream, the  $\text{HCO}_3^-$  in the downstream, and the  $\text{Ca}^{2+}$  and  $\text{Mg}^{2+}$  were the controlling ions (accounting for >50% of the total anions/cations) in the Chaiqu watershed. Stoichiometry and principal component analysis (PCA) results revealed that sulfuric acid stimulated the weathering of carbonates and silicates to produce riverine solutes. This study promotes understanding water source dynamics to inform water quality and environmental management in alpine regions.

## 1. Introduction

Rivers are closely connected with the biosphere, pedosphere, and atmosphere. The riverine chemical compositions generally carry the environmental information about the regional hydrological cycle (Mokarram et al., 2022; Xiao et al., 2022). The Tibet Plateau (TP), often referred to as the “Asian water tower” due to its plentiful water sources, supports billions of people (Li et al., 2021). The Yarlung Tsangpo River (YTR), being the highest large river on a global scale, also contains the greatest drainage area in the TP, sustaining scientific concern about regional hydrological processes (Li et al., 2021; Wang et al., 2022). Rivers in the TP are quite sensitive to environmental alterations (Xuan et al., 2021). The differences in population density along the YTR are enormous (Zhang et al., 2022a). The majority of studies focused on the water quality assessment in the densely populated downstream locations of YTR (Bai et al., 2014; Hren et al., 2007; Zhu et al., 2021). The hydrochemistry of the YTR’s headwaters with low population density is poorly understood, particularly in the alpine region. By estimating the

anthropogenic impact with a sparse population, the hydrochemical compositions can better reflect the environmental changes in alpine rivers, which can strengthen the hydrological process clarification on a regional scale.

The riverine solute compositions have been widely applied to construct the dynamic hydrological cycle between precipitation, runoff, and groundwater (Liu et al., 2022b; Ren et al., 2017; Zhao et al., 2019). Identification of solute sources is achieved using multiple methods, such as principal component analysis (PCA) and stoichiometry methods (Li et al., 2020; Liu and Han, 2020; Zeng et al., 2023). In addition, the Global Network of Isotopes in Rivers (GNIR) and Global Meteoric Water Line (GMWL) have been already established to identify different processes of the hydrological cycle (Craig, 1961; Halder et al., 2015). Therein  $\delta^2\text{H}$  and  $\delta^{18}\text{O}$  are widely considered naturally sensitive tracers for various regional hydrological processes (e.g., evaporation and water mixing, etc.) (Li et al., 2022; Yang and Han, 2020; Zhao et al., 2019). The weaker rainfall and strong evaporation generally increase the  $\delta^{18}\text{O}$  values of river water (Li et al., 2021). Large variations of  $\delta^{18}\text{O}$  value

\* Corresponding author. No. 19 Beitucheng West Road, Chaoyang District, Beijing, 100029, China.

E-mail address: [zfxu@mail.igcas.ac.cn](mailto:zfxu@mail.igcas.ac.cn) (Z. Xu).

ranges (>20%) have also been found between the dry and wet seasons in the YTR (Shi et al., 2021a). The combined approach of major ions,  $\delta^{2\text{H}}$ , and  $\delta^{18\text{O}}$  may be informative to decipher the mixing, evolution, and fate of river water and solute.

Most studies mainly revolved around the spatio-temporal variations of solutes in the YTR or the source region of Yangtze, Lancang, and Nu rivers in the TP (Jiang et al., 2022; Liu et al., 2022a; Qu et al., 2015; Zhang et al., 2019). However, complex lithology, variable climate, and anthropogenic disturbance continue the challenge to distinguish the riverine solute sources and regulating mechanisms of hydrological characteristics on a large scale (Xuan et al., 2021; Zeng et al., 2022). In contrast, the similar geological background in the small watersheds makes information simplified to easily decipher the influence of weathering and different contributors of components (Han et al., 2023; Jiang et al., 2018; Liu et al., 2023). The Chaiqu watershed locates in the southwest of the TP, holding the headwaters of YTR. This study combining analyzed major ions and stable isotopic compositions to (1) determine the hydrogeochemical characteristics in the headwater of YTR; (2) discuss the potential sources of riverine components and the controlling factors that are responsible for the  $\delta^{2\text{H}}$  and  $\delta^{18\text{O}}$  fractionations; (3) explore the influences of hydrological dynamics and water sources in the alpine rivers.

## 2. Materials and methods

### 2.1. Study area

The study area is located at the northern foothills of the Himalaya Mountain, southwestern TP ( $29^{\circ}42' - 29^{\circ}53' \text{N}$ ,  $84^{\circ}02' - 84^{\circ}25' \text{E}$ ) (Fig. 1). The Chaiqu watershed is occupied by most grassland and rarely disturbed by human activities. Additionally, the total dissolved solids (TDS) and water temperature of the surface water in the YTR are both low (Huang et al., 2009). Located in a typical high-altitude (>4500 m) watershed, the Chaiqu watershed is controlled by a temperate semiarid monsoon climate (Li et al., 2020). The dry season is dominated by subpolar westerlies from October to May next year, while the wet season is controlled by the South Asian monsoon from June to September (Liu et al., 2022b). The temperature during summer is from  $7.1^{\circ}\text{C}$  to  $18.5^{\circ}\text{C}$  in Tibet, showing a significant upward trend in recent years (Gao et al., 2020; Tang et al., 2021). More than 90% of precipitation is concentrated from June to September with annual precipitation of 413 mm and annual evaporation of 2298 mm in southwestern TP (Shi et al., 2021b). The study area is widely distributed with Quaternary sediments and Cenozoic granitoid (Shi et al., 2021a).

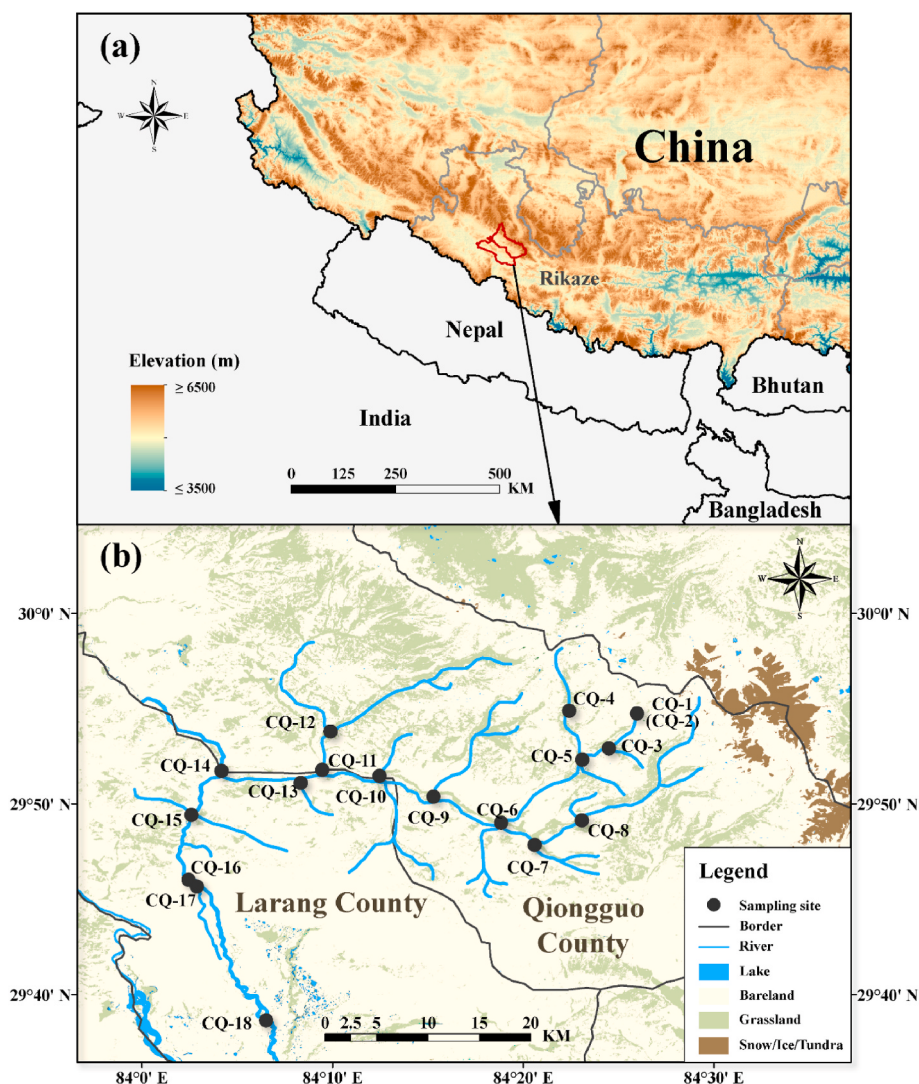


**Fig. 1.** Sampling sites and land-use types in the Chaiqu watershed. (a) the Digital Elevation Model (DEM) map of the study area; (b) land-use types and sampling sites in the study area.

## 2.2. Sampling and hydrogeochemical parameter analyses

An analysis of 17 river water samples and one grass water sample (CQ-2) was conducted based on the regional lithology and land uses from the Chaiqu watershed, located in the upper reaches of YTR in May 2018 (before the high flow, Fig. 1). Due to weak effects of dilution by small runoff volume in the dry season, water samples can better reflect the solute composition to understand the water cycle and chemical weathering processes. The electrical conductivity (EC)/pH meter (HANNA-HI98129, Italy) was applied to measure EC and pH in water, and the TDS values were calculated by half values of EC. Each water sample through a cellulose-acetate membrane filter (0.22 µm, Millipore) was stored in polyethylene bottles. And all bottles were pre-soaked with Milli-Q water (18.2 MΩ·cm). Titration of  $\text{HCO}_3^-$  concentrations was conducted within 12 h using pre-calibrated HCl. Other anions ( $\text{F}^-$ ,  $\text{Cl}^-$ ,  $\text{NO}_3^-$ ,  $\text{SO}_4^{2-}$ ) were determined by Ion Chromatograph (IC, DIONEX, ICS-1500, USA), and cations ( $\text{Na}^+$ ,  $\text{K}^+$ ,  $\text{Mg}^{2+}$ ,  $\text{Ca}^{2+}$ ) were measured by Inductively Coupled Plasma Optical Emission Spectrometer (ICP-OES, IRIS Intrepid II XSP, USA). All analyses were of the relative standard deviations within ±5%. All samples were repeatedly measured and the procedural blank was employed for quality control. The measurements were completed at the Key Laboratory of Cenozoic Geology and Environment, Institute of Geology and Geophysics, Chinese Academy of Sciences (CAS).

## 2.3. Isotope measurement

The stable isotopes of H and O were analyzed by Water Isotope Analyzer (PICARRO L1102-i USA), with the analytical precision of ±0.5‰ for  $\delta^2\text{H}$  and ±0.1‰ for  $\delta^{18}\text{O}$ . Replicate samples and procedural blanks were used to ensure quality control. All isotopic ratios were reported in per mill (‰), and the measurements of  $\delta^2\text{H}$  and  $\delta^{18}\text{O}$  were normalized to the ratios of international Vienna Standard Mean Ocean Water (V-SMOW). The final results were determined by averaging three measurements made for each sample. The kinetic disequilibrium fractionation of  $\delta^2\text{H}$  and  $\delta^{18}\text{O}$  may appear during water evaporation, causing the variation of  $\delta^2\text{H}$  and  $\delta^{18}\text{O}$  (Craig, 1961), which was defined as deuterium excess (d-excess) (Dansgaard, 1964). The formulas of  $\delta^2\text{H}$ ,  $\delta^{18}\text{O}$ , and d-excess calculations were presented as follows (Das et al., 2020):

$$\delta^{18}\text{O} = \left[ \left( ^{18}\text{O}/^{16}\text{O} \right)_S / \left( ^{18}\text{O}/^{16}\text{O} \right)_{ST} - 1 \right] \times 1000 \quad (1)$$

$$\delta^2\text{H} = \left[ \left( ^2\text{H}/^{1\text{H}} \right)_S / \left( ^2\text{H}/^{1\text{H}} \right)_{ST} - 1 \right] \times 1000 \quad (2)$$

$$\text{d-excess} = \delta^2\text{H} - 8 \times \delta^{18}\text{O} \quad (3)$$

where the S represents the sample, and the ST represents the values of V-SMOW standard. The duplicate measurements were performed on each sample to ensure accuracy.

## 2.4. Data statistics processing

The component analyses were completed by the statistics software package of SPSS 25.0 (IBM SPSS Statistics, Chicago, IL, USA) based on the values of ions and isotopes. Graphics were drawn by Origin (2017) (OriginLab, Northampton, UK), and improved by Adobe Illustrator CC 2018.

## 3. Results

### 3.1. Hydrochemistry of waters

The parameters of water samples were summarized in Table 1, and

**Table 1**

Variations of riverine composition and related parameters in the Chaiqu watershed.

Parameters	Min	Max	Mean	SD	Chinese Guideline	WHO Guideline
T (°C)	0.2	17.2	8.4	4.6	–	–
pH	6.8	8.7	8.0	0.5	6.5–8.5	6.5–8.5
DO (mg/L)	1.70	3.60	2.47	0.48	–	–
TDS (mg/L)	90	306	174.94	61.55	–	–
$\text{Na}^+$ (mg/L)	1.73	66.30	14.17	17.95	–	–
$\text{K}^+$ (mg/L)	0.50	2.72	1.33	0.66	–	–
$\text{Mg}^{2+}$ (mg/L)	1.81	28.63	9.16	6.27	–	–
$\text{Ca}^{2+}$ (mg/L)	16.41	96.41	52.36	16.79	–	–
$\text{F}^-$ (mg/L)	0.12	1.02	0.32	0.23	0.95	1.52
$\text{Cl}^-$ (mg/L)	1.56	42.65	10.85	10.78	249.94	249.94
$\text{NO}_3^-$ (mg/L)	0.62	2.98	2.08	0.57	89.40	223.50
$\text{SO}_4^{2-}$ (mg/L)	6.28	260.99	81.95	73.17	249.77	249.77
$\text{HCO}_3^-$ (mg/L)	61.72	177.90	132.62	35.94	–	–
$\delta^2\text{H}$ (‰)	-145.3	-126.3	-141.4	4.55	–	–
$\delta^{18}\text{O}$ (‰)	-19.6	-15.6	-18.6	0.89	–	–
d-excess (‰)	-6.4	6.9	1.5	3.01	–	–

the raw data were listed in Table A1. The water temperature varied from 0.2 °C to 17.2 °C. The TDS varied from 90 to 306 mg/L, which basically showed a decreasing trend down the river flows. The mean value of TDS was 174.9 mg/L in the Chaiqu watershed, which was lower than that in the Nianchu River (203.5 mg/L) (Shi et al., 2021a) and Naqu River (271.0 mg/L) (Wang et al., 2019), but higher than the average of Asian rivers (142.0 mg/L) and the global level (120.0 mg/L) (Huang et al., 2011). The river water was slightly alkaline with pH values ranging from 6.8 to 8.7 (average 8.0). The normalized inorganic charge balance (NICB,  $[\text{TZ}^+ \cdot \text{TZ}^-]/[\text{TZ}^+]$ ) ranged from -12.25% to 7.13% (mean value: -4.56%), indicating that the cation and anion in the Chaiqu watershed were basically balanced. The dominant cation was  $\text{Ca}^{2+}$  (contained >50% of the total cations in 16 water samples) and the dominant anion was  $\text{HCO}_3^-$  (contained >50% of the total anions in 11 water samples) or  $\text{SO}_4^{2-}$  (accounted for >50% of the total anions in 6 water samples) in rivers of the Chaiqu watershed. Therefore, the compositions of major ions were divided into two hydrochemical types (Fig. 2). The first group of the river waters (10 samples) in the Chaiqu watershed exhibited similar hydrogeochemical compositions of  $\text{HCO}_3^- \cdot \text{Ca} \cdot \text{Mg}$  type to that of the main channel YTR (Huang et al., 2011). While the other water samples (7 samples) in the Chaiqu watershed were similar to the well water in the Lhasa (Zhang et al., 2018) and groundwater in the Rikaza City (Li et al., 2020) of  $\text{SO}_4^{2-} \cdot \text{Cl}^- \cdot \text{Ca} \cdot \text{Mg}$  type. Additionally, the hydrogeochemical compositions of two river waters in the Chaiqu watershed were evidently with high  $\text{Na}^+$  and  $\text{K}^+$  concentrations.

### 3.2. Spatial distribution of riverine composition

The variations of major ions in the rivers of Chaiqu watershed are plotted in Fig. 3a and 3b, and all detailed data are listed in Table A1. From the perspective of the whole watershed, the  $\text{K}^+$  and  $\text{Mg}^{2+}$  concentrations were generally stable. The concentrations of  $\text{Ca}^{2+}$  occupied the highest proportion in that of the total cation in most river waters, excluding the CQ-4 and CQ-6 dominated by  $\text{Na}^+$  (contained >50% in total cation concentrations). The higher  $\text{Na}^+$  concentration at CQ-6 ( $\text{Na}^+$  value: 60.67 mg/L) may result from an import of tributary where CQ-4 ( $\text{Na}^+$  value: 66.30 mg/L) was located. The  $\text{Cl}^-$  concentrations ranged from 1.56 mg/L to 42.65 mg/L, and the concentration variation of  $\text{Cl}^-$  in flow was similar to that of  $\text{Na}^+$ . The  $\text{SO}_4^{2-}$  concentrations obviously

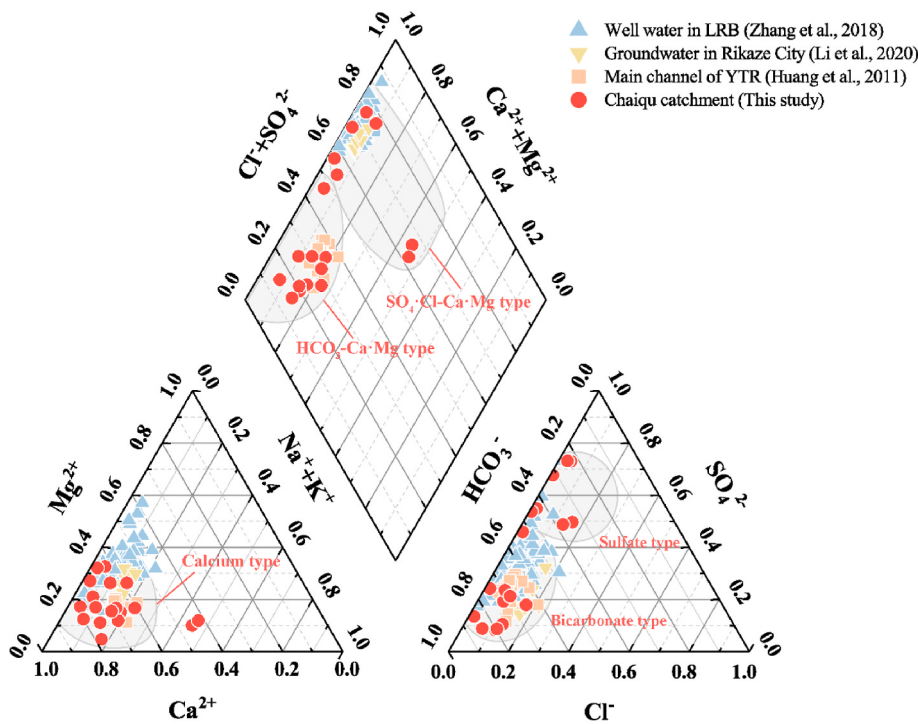
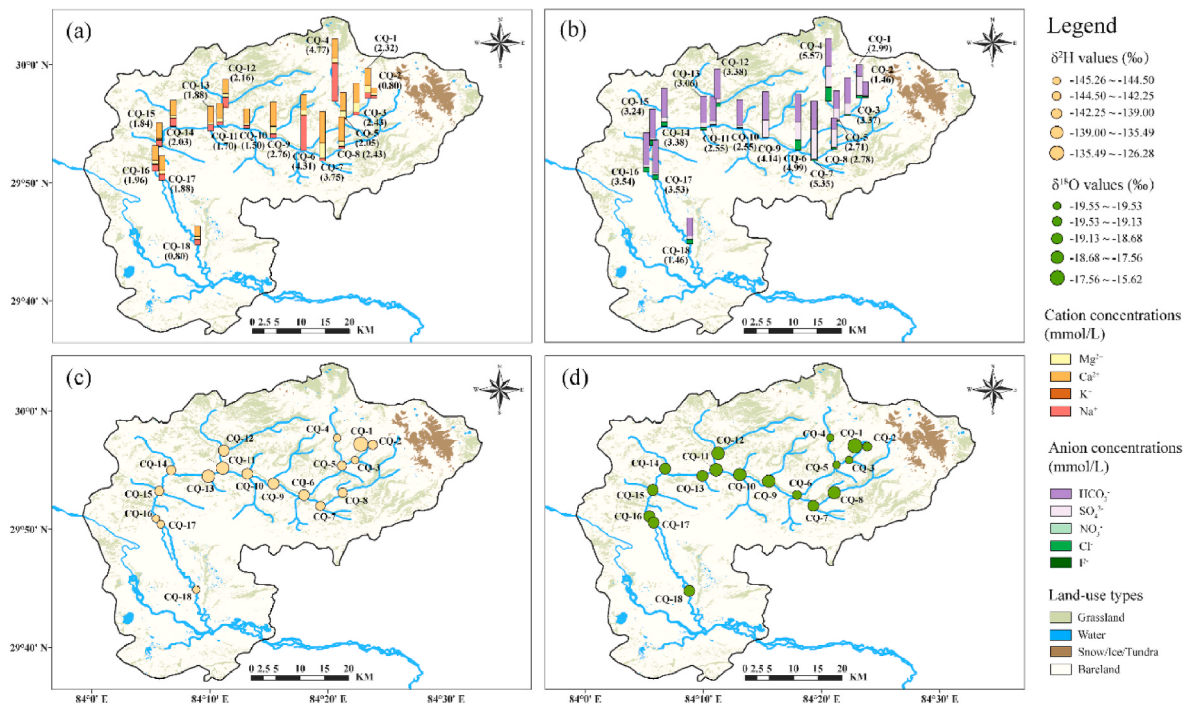


Fig. 2. Piper plot of dissolved major ions in rivers.

Fig. 3. Spatial variation of major ions,  $\delta^2\text{H}$ , and  $\delta^{18}\text{O}$  in the Chaiqu watershed (a) total cation concentrations and percentage of each anion, (b) total anion concentrations and percentage of each cation, (c) values of  $\delta^2\text{H}$ , and (d) values of  $\delta^{18}\text{O}$ .

decreased while the  $\text{HCO}_3^-$  concentrations showed an increasing trend in river water where several tributaries converged. The variations of  $\text{F}^-$  and  $\text{NO}_3^-$  concentrations were limited in the whole Chaiqu watershed. Results showed that the  $\delta^2\text{H}$  values ranged from  $-126.3\text{\textperthousand}$  to  $-145.3\text{\textperthousand}$  with an average of  $-141.4\text{\textperthousand}$ . The  $\delta^{18}\text{O}$  values ranged from  $-19.6\text{\textperthousand}$  to  $-15.6\text{\textperthousand}$  with an average of  $-18.6\text{\textperthousand}$ . The trends for  $\delta^2\text{H}$  and  $\delta^{18}\text{O}$  showed an increase upstream while a decrease downstream, excluding

CQ-2, a sample originating from grassland (Fig. 3c and 3d). The d-excess ranged from  $-2.2\text{\textperthousand}$  to  $6.9\text{\textperthousand}$  in the river, which showed a decreasing trend with the flow, and in  $-6.4\text{\textperthousand}$  of grass water.

## 4. Discussion

### 4.1. Source identification of riverine solutes

#### 4.1.1. PCA analysis

The PCA analysis is frequently employed to explore the sources of riverine solutes (Ogwueleka, 2014). In this study, four principal components (PCs) contained 86.72% of the total variance (PC1: 33.94%, PC2: 27.04%, PC3: 16.11%, and PC4: 9.63%), and the eigenvalues of three PCs were higher than 1 in the rivers of Chaiqu watershed (Table 2). PC1 had high positive loadings ( $>0.65$ ) of  $Mg^{2+}$ ,  $Ca^{2+}$ ,  $SO_4^{2-}$ , TDS, and EC. Both the weathering of carbonate and silicate rocks could provide plenty of  $Ca^{2+}$  and  $Mg^{2+}$ . Noteworthy, the contributions of dissolved  $Ca^{2+}$  and  $Mg^{2+}$  from carbonate minerals could reach above 80% in the Tibetan rivers, even in the area dominated by silicate rocks (Hren et al., 2007; Wu et al., 2008). Generally, the weathering of carbonate and silicate rocks will also release abundant  $HCO_3^-$  while producing  $Ca^{2+}$  and  $Mg^{2+}$ . Although the  $HCO_3^-$  in PC1 had positive loading, the value was only 0.24, suggesting that the riverine  $HCO_3^-$  was possibly contributed by other sources, or that other  $Ca^{2+}$  and  $Mg^{2+}$  sources were interfering with the composition analysis. The higher loading of  $SO_4^{2-}$  in PC1 may indicate the involvement of sulfuric acid in rock weathering. Combined with the analysis above, PC1 might be regarded from carbonate weathering and was mainly influenced by sulfuric acid. PC2 consisted of  $Na^+$ ,  $K^+$ , and  $Cl^-$  with a strong loading ( $>0.90$ ). It has been reported that abundant  $Na^+$  and  $K^+$  would be released by the weathering of silicates in the Tibetan rivers, especially in the dry season with slow velocity (Jiang et al., 2015; Li et al., 2016). In addition, riverine  $Cl^-$  is commonly considered to derive from halite dissolution accompanied by equivalent levels of  $Na^+$  or groundwater inputs in the area of limited human activities (Huang et al., 2011). The common location of  $Na^+$  and  $Cl^-$  may demonstrate that they have one same source at least. It can be concluded that PC2 represented the influence of silicate weathering and halite dissolution or groundwater inputs.

And the pH,  $F^-$  and  $NO_3^-$  from PC3 have only loading 16.11% variance in river waters. The high levels of  $F^-$  and  $NO_3^-$  concentrations are commonly regarded as symbols of human inputs (Jiang et al., 2021; Zhang et al., 2022b). However, the concentrations of  $F^-$  and  $NO_3^-$  were lower than 0.05 mmol/L in river of the Chaiqu watershed, which indicated that the water environment was undisturbed by human activities. This is consistent with sparse human activity in the study area. The PC4 only had high loading of DO with the eigenvalue of 0.95, which may represent the influence of the physical parameters. It is noteworthy that the  $HCO_3^-$  did not show an evident tendency in each PC (the loading was less than 0.5), indicating that the complex sources. The ratios of  $HCO_3^-$  versus  $(HCO_3^- + SO_4^{2-})$  were determined to indicate the proton source

(Pant et al., 2018). A value higher than 0.5 represents the primary proton source of atmospheric  $CO_2$ , while a value lower than 0.5 represents that carbonate weathering with sulfuric acid dominates the contribution (Pant et al., 2018). The upstream river water (CQ-1 to CQ-9) exhibited the  $[HCO_3^-]/(HCO_3^- + SO_4^{2-})$  ratios ( $0.35 \pm 0.11$ ) of less than 0.5 except for CQ-3 (0.53). And the values in downstream rivers (CQ-10 to CQ-18,  $0.83 \pm 0.08$ ) were close to 1 in the study area. Therefore, weathering processes in the Chaiqu watershed may be controlled by sulfuric acid in the upper reach and carbonic acid in the lower reach. Overall, the riverine components in the Chaiqu watershed were mainly contributed by the weathering of carbonates and silicates with strong effects of sulfuric acid, and possibly evaporative dissolution.

#### 4.1.2. Rock weathering processes

Several studies proposed that the hydrochemistry of rivers in the TP was controlled by intensive weathering and erosion rather than anthropogenic inputs (Huang et al., 2009; Ren et al., 2016). To determine the contribution of riverine solutes, the stoichiometry analyses were applied to the river waters in the Chaiqu watershed and compared with those in other Tibetan rivers (Fig. 4). The Na normalized elemental ratios were applied to eliminate the disturbance of dilution and evaporation (Gaillardet et al., 1999). And the dominant reaction of weathering can be explored based on ratios of  $Ca^{2+}/Na^+$  versus  $HCO_3^-/Na^+$  (Gaillardet et al., 1999). A large proportion of samples from the Chaiqu watershed were distributed between the end-members of silicate and carbonate (Fig. 4a), indicating that the hydrochemistry in the Chaiqu watershed was affected by the weathering of carbonates and silicates (Jiang et al., 2015; Zhang et al., 2018). The contribution from the carbonate minerals for solutes in the Chaiqu watershed was larger than that in the main channel of the upper and middle reaches of YTR, while similar to that in the well waters in Lhasa (Jiang et al., 2015; Zhang et al., 2018). This is consistent with the carbonate and silicate weathering-dominated river compositions in previous studies (Jiang et al., 2015; Wang et al., 2020). In addition, the samples of CQ-4 and CQ-6 were relatively closer to the evaporite end-member, which possibly resulted from high concentrations of  $Na^+$ . CQ-6 was in the lower reach of CQ-4, thus the riverine solutes in CQ-6 may be influenced by the tributary where CQ-4 was located. Generally, high levels of  $Na^+$  and  $Cl^-$  concentrations in rivers may be contributed to salt lakes, high-mineral springs, or evaporate dissolution (Huang et al., 2011). Based on the field survey, there are no salt lakes or exposed springs adjacent to the river segment of CQ-4 and CQ-6. Therefore, the deeper groundwater or halite dissolution release may become the primary source of  $Cl^-$ . The dissolution of halite generally releases abundant  $Na^+$  and  $Cl^-$  with  $Na/Cl$  molar ratios of 1 (Yang et al., 2016). However, the molar ratios between  $Na^+$  and  $Cl^-$  were almost much greater than 1 in all samples (except for the value of CQ-18 was 0.98), which indicated that the halite may not be the main source of  $Na^+$  (e.g., silicate weathering). Besides the weathering of silicates that can release  $Na^+$ , the release of  $Na^+$  and  $K^+$  from the rocks will exchange with the  $Ca^{2+}$  and  $Mg^{2+}$  from the solution (Li et al., 2016; Marghade et al., 2012). The  $K^+$  concentrations also showed relatively high levels in CQ-4 and CQ-6. Moreover, the ratios of  $(Na^++K^+)/Cl^-$  were higher than 1 in all samples (Fig. 5). Therefore, halite dissolution and cation exchange between minerals and solution may influence the additional  $Na^+$  in river waters in the Chaiqu watershed.

To further determine the contributions from carbonate and silicate minerals, the ratios of  $[(Ca^{2+}+Mg^{2+})/HCO_3^-]$  versus  $[(Na^++K^+)/HCO_3^-]$  were calculated (Fig. 4b). Line 1 represents an ideal weathering process that all major cations were released from rock by carbonic acid; line 2 means the equal contribution of silicate and carbonate minerals with entire  $Ca^{2+}$  and  $Mg^{2+}$  from carbonate minerals; while the line 3 means the silicate minerals contribute twice as much as carbonate minerals with part of  $Ca^{2+}$  and  $Mg^{2+}$  from the dissolution of carbonate minerals (50%) (Liu and Han, 2020). Most samples located below line 3 presented the high contribution of river solutes from silicate minerals due to higher

**Table 2**

Varimax-rotated component matrix for ions in river waters draining through the Chaiqu watershed.

Variable	PC 1	PC 2	PC 3	PC 4	Communalities
pH	0.35	0.05	<b>-0.56</b>	0.32	0.54
TDS	<b>0.85</b>	0.29	-0.38	-0.04	0.95
DO	-0.20	0.35	0.09	<b>0.89</b>	0.96
EC	<b>0.85</b>	0.29	-0.38	-0.04	0.95
$Na^+$	0.22	<b>0.91</b>	0.20	-0.10	0.94
$K^+$	-0.04	<b>0.90</b>	-0.02	-0.14	0.83
$Mg^{2+}$	<b>0.80</b>	-0.42	0.33	0.08	0.93
$Ca^{2+}$	<b>0.68</b>	-0.40	0.49	0.05	0.87
$F^-$	-0.13	-0.08	0.30	-0.05	0.12
$Cl^-$	0.04	<b>0.96</b>	0.18	-0.10	0.97
$NO_3^-$	-0.47	0.39	<b>0.59</b>	-0.08	0.74
$SO_4^{2-}$	<b>0.75</b>	-0.04	0.63	0.10	0.96
$HCO_3^-$	<b>0.24</b>	0.14	-0.20	-0.43	0.30
Eigenvalues	3.33	2.65	1.58	0.95	
Variance (%)	33.94	27.04	16.11	9.63	
Cumulative (%)	33.94	60.98	77.09	86.72	

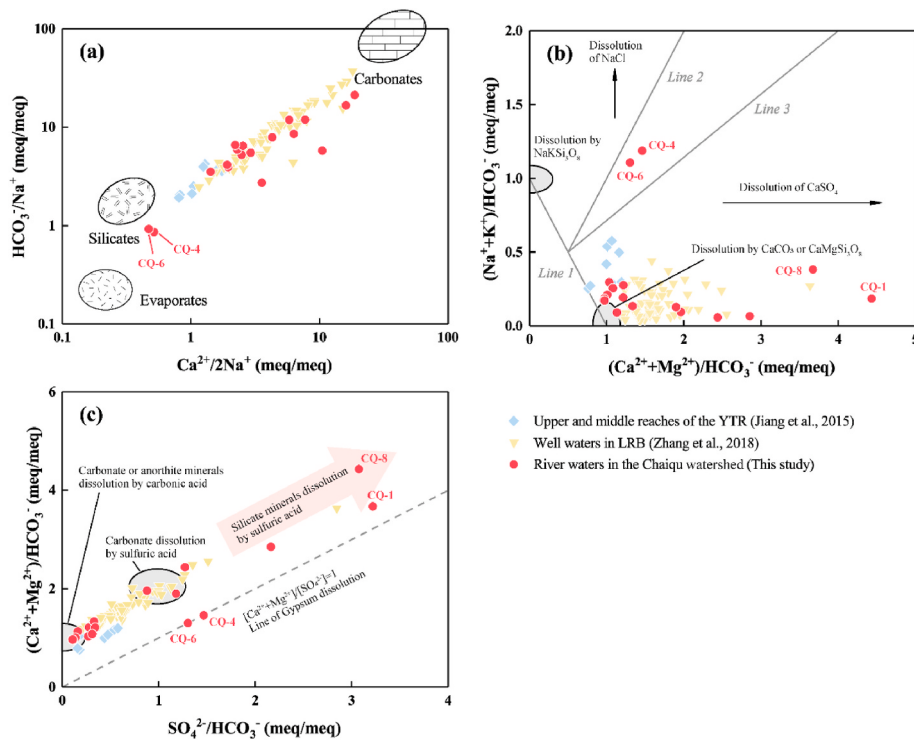


**Fig. 4.** Contributors determination of riverine components in the Tibetan rivers. (a)  $[\text{Ca}^{2+}/\text{Na}^+]$  versus  $[\text{HCO}_3^-/\text{Na}^+]$ , (b)  $[(\text{Ca}^{2+}+\text{Mg}^{2+})/\text{HCO}_3^-]$  versus  $(\text{Na}^++\text{K}^+)/\text{HCO}_3^-$ , and (c)  $[\text{SO}_4^{2-}/\text{HCO}_3^-]$  versus  $[(\text{Ca}^{2+}+\text{Mg}^{2+})/\text{HCO}_3^-]$ .

Sampling sites		CQ-1	CQ-2	CQ-3	CQ-4	CQ-5	CQ-6	CQ-7	CQ-8	CQ-9
ion ratios (meq/meq)		2.02	2.12	2.94	2.46	1.41	3.04	2.18	1.49	7.45
	$(\text{Na}^++\text{K}^+)/\text{Cl}^-$	2.60	0.67	1.29	1.19	1.76	1.01	1.91	3.63	1.47
	$\text{Ca}^{2+}/\text{HCO}_3^-$	3.67	0.97	1.96	1.46	2.44	1.30	2.85	4.43	1.90
	$(\text{Ca}^{2+}+\text{Mg}^{2+})/(\text{HCO}_3^-+\text{SO}_4^{2-})$	0.87	0.88	1.04	0.59	1.07	0.57	0.90	1.09	0.87
Sampling sites		CQ-10	CQ-11	CQ-12	CQ-13	CQ-14	CQ-15	CQ-16	CQ-17	CQ-18
ion ratios (meq/meq)		4.36	5.65	2.44	1.90	1.77	1.27	1.30	1.17	1.07
	$(\text{Na}^++\text{K}^+)/\text{Cl}^-$	0.98	1.08	0.81	1.06	0.92	0.95	0.77	0.78	0.99
	$\text{Ca}^{2+}/\text{HCO}_3^-$	1.13	1.33	1.03	1.21	1.08	1.01	0.97	0.96	1.22
	$(\text{Ca}^{2+}+\text{Mg}^{2+})/(\text{HCO}_3^-+\text{SO}_4^{2-})$	0.97	1.00	0.81	0.91	0.82	0.88	0.88	0.86	0.95

**Fig. 5.** Ion ratios of riverine solutes in the study area.

values of  $[(\text{Ca}^{2+}+\text{Mg}^{2+})/\text{HCO}_3^-]$ , which is considered an extreme weathering process. The greatly high values of  $[(\text{Ca}^{2+}+\text{Mg}^{2+})/\text{HCO}_3^-]$  ( $>2$ ) should be attributed to the strong involvement of sulfuric acid in rock weathering (Liu and Han, 2020). Co-occurring materials in silicate and carbonate rocks may disturb this artifact, as well as gypsum dissolution (Hren et al., 2007). High values of  $[(\text{Ca}^{2+}+\text{Mg}^{2+})/\text{HCO}_3^-]$  suggest that the dissolution of  $\text{CaSO}_4$  could increase the concentration of  $\text{Ca}^{2+}$ . The obviously high level of  $\text{Ca}^{2+}$  and  $\text{SO}_4^{2-}$  were also found in the upper reach, especially in CQ-7 and CQ-8. The dissolution of evaporite usually

has a strong correlation between  $\text{SO}_4^{2-}$  and  $\text{Cl}^-$  (Wu et al., 2008), whereas it did not occur in the river waters of the Chaiqu watershed. Therefore, it can only be determined that sulfuric acid was strongly involved in the weathering of the upstream, whether the source of sulfide oxidation or regional gypsum dissolution should be further discussed.

Based on the weathering of carbonate exposed to carbonic acid and sulfuric acid, the ratios of  $\text{SO}_4^{2-}/\text{HCO}_3^-$  versus  $[(\text{Ca}^{2+}+\text{Mg}^{2+})/\text{HCO}_3^-]$  were applied to determine mixing processes (Fig. 4c). And the variations

of ion ratios are listed in Fig. 5. The results showed that river waters in the lower reach of the Chaiqu watershed were affected by the carbonate dissolution with carbonic acid, which was similar to those in the YTR. It is notable that the ratios of  $[(\text{Ca}^{2+} + \text{Mg}^{2+})/\text{HCO}_3^-]$  are similar in the weathering by the carbonic acid of anorthite ( $\text{CaAl}_2\text{Si}_2\text{O}_8$ ) or carbonate minerals ( $\text{Ca}_{x}\text{Mg}_{(1-x)}\text{CO}_3$ ). Perhaps this may explain why the data points in this study tended to the end-member of carbonate minerals dissolution by carbonic acid. According to the comprehensive analyses of  $\text{Ca}^{2+}/\text{HCO}_3^-$  ratios in the upper reach of the Chaiqu watershed (Fig. 5),  $\text{HCO}_3^-$  was basically balanced by  $\text{Ca}^{2+}$ , indicating the dominant contributor of carbonate minerals. Moreover, the obviously higher levels of  $\text{Ca}^{2+}$  than  $\text{HCO}_3^-$  suggested that the weathering of rocks was strongly affected by other acids. The assumption of sulfide acid can also be reflected based on the ratios of  $(\text{Ca}^{2+} + \text{Mg}^{2+})/(\text{HCO}_3^- + \text{SO}_4^{2-})$ . The values of  $\text{Ca}^{2+}/\text{HCO}_3^-$  lower than 1 and  $(\text{Ca}^{2+} + \text{Mg}^{2+})/(\text{HCO}_3^- + \text{SO}_4^{2-})$  higher than 1 concentrated in the lower reaches of river, indicating the weathering of silicate minerals and the limited influence of sulfide acid. Generally, the  $\text{SO}_4^{2-}$  in natural rivers is produced by the sulfide mineral (e.g., pyrite, and  $\text{FeS}_2$ ) oxidation or the dissolution of evaporites (Han and Liu, 2004). Due to the no existence of springs around sampling sites, it can be speculated that  $\text{SO}_4^{2-}$  in the area may be contributed to deeper groundwater flow through the gypsum layer or sulfidic oxidation. However, according to the geological maps published by the government, there is no distribution of evaporites in the surface layer of the study area. Wang et al. (2020) also suggested that  $\text{SO}_4^{2-}$  mainly originated from pyrite oxidation in the YTR basin. Therefore, the observations from the Chaiqu watershed suggested that  $\text{SO}_4^{2-}$  in the river was possibly mostly derived from the sulfide minerals oxidation. Overall, riverine solutes in the Chaiqu watershed were mainly contributed by carbonate minerals, and parts of  $\text{Ca}^{2+}$  and  $\text{Mg}^{2+}$  were released by silicate minerals (especially downstream). The weathering process involved a combination of carbonic acid and sulfuric acid, and sulfuric acid mainly took effect in the upper reach. In addition, the  $\text{Na}^+$  and  $\text{Cl}^-$  were released by halite dissolution, while  $\text{K}^+$  and additional  $\text{Na}^+$  were mainly contributed by weathering of silicate.

#### 4.2. Isotope-based recharge sources identification

##### 4.2.1. Riverine isotope compositions

The application of  $\delta^2\text{H}$  and  $\delta^{18}\text{O}$  are wildly used to explore river water sources (e.g., glacier meltwater, precipitation, and groundwater) (Gammons et al., 2006; Yang and Han, 2020). The sources of riverine solutes were determined by the analyses of dissolved major ions, and the values of  $\delta^2\text{H}$  and  $\delta^{18}\text{O}$  were further employed to identify the water

recharge sources (Fig. 6). The  $\delta^2\text{H}$  and  $\delta^{18}\text{O}$  from atmospheric precipitation basically followed the linear correlation by the Global Meteoric Water Line (GMWL):  $\delta^2\text{H} = 8 * \delta^{18}\text{O} + 10\%$  (Craig, 1961). Most surface waters in the TP were located at the bottom right of GMWL, which also applied to that in the Chaiqu watershed (>75% of samples located at the bottom right of GMWL, Fig. 6a). All samples in the Chaiqu watershed were located at the bottom right of the Local Meteoric Water Line (LMWL) in the TP (Liu et al., 2014). The lower intercept of LWML in the TP than that of GMWL is attributed to the influence of the regional water cycle and atmosphere transport. The lower slope was also found in the  $\delta^2\text{H}-\delta^{18}\text{O}$  line of the Rikaze precipitation from April to May (Shi et al., 2021a). The strong seasonal variability of the recharge contributor possibly dominated the  $\delta^2\text{H}$  and  $\delta^{18}\text{O}$  composition. The  $^{18}\text{O}$ -depleted precipitation generally occurred from June to September by Indian monsoon, while the westerly derivation carried higher values of  $\delta^2\text{H}$  and  $\delta^{18}\text{O}$  in precipitation during winter (Dai et al., 2021; Liu et al., 2007). Thus, the maximal values of  $\delta^2\text{H}$  and  $\delta^{18}\text{O}$  in Tibetan rivers always occur from May to June in a year. Besides rainfall, the contribution from precipitation may also turn into the form of dry deposition, and the snow is remarkably enriched in heavier isotopes than the ice even in winter and spring (Tian et al., 2020). Overall, the seasonal change in moisture source and dry deposition may induce the heavier isotopic composition in rivers of the Chaiqu watershed.

The blank line represents the GMWL in (a). The dark-grey line represents the correlation between the altitude and d-excess values, the light-grey dotted line represents the correlation between the altitude and  $\delta^{18}\text{O}$  values, and the grey spots represent values of CQ-2 (grass water) in (b).

Assuming that the isotopic composition in precipitation governs the spatial isotopic composition in river water, it follows that the  $\delta^2\text{H}$  and  $\delta^{18}\text{O}$  values would exhibit a decreasing trend downstream (Tan et al., 2021). However, this variation was not observed in the study area (Fig. 2), suggesting that the river had other recharge sources or experienced evaporation. In regions characterized by high evaporation and low precipitation, kinetic fractionation possibly arises from the varying diffusion rates of water molecules with different hydrogen and oxygen isotope ratios (Craig, 1961). The slope of  $\delta^2\text{H}-\delta^{18}\text{O}$  line may decrease during the process of isotopic enrichment. The linear correlation between  $\delta^2\text{H}$  and  $\delta^{18}\text{O}$  showed  $\delta^2\text{H} = 4.79 (\pm 0.44) * \delta^{18}\text{O} - 52.2 (\pm 8.13)\%$  ( $R^2 = 0.88$ ) in rivers of the Chaiqu watershed, which was closed to that line of rivers (the slope of 5.77) and lakes (the slope of 5.27) with stronger evaporation in the TP (Tan et al., 2014). According to the calculations based on the Craig-Gordon model, the slope of  $\delta^2\text{H}$  and  $\delta^{18}\text{O}$  relationship in surface waters will extremely decrease (<4.5) in the

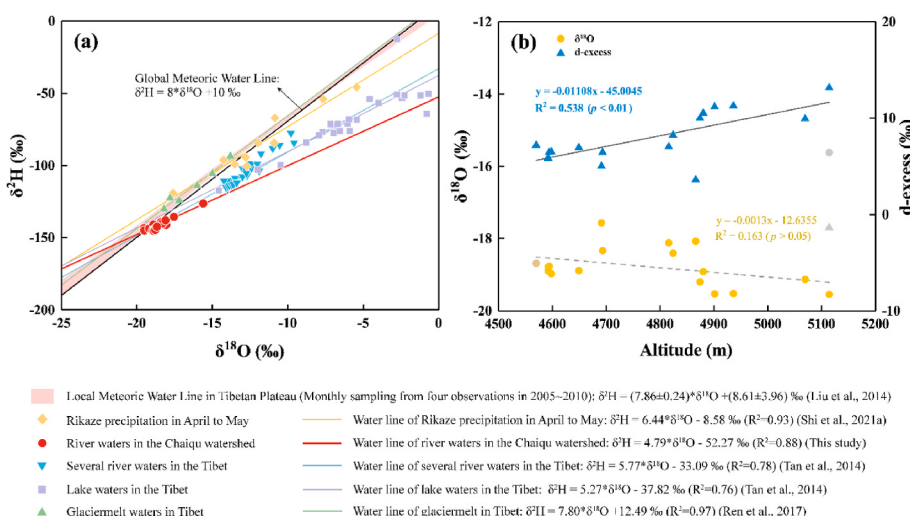


Fig. 6. Relationships among  $\delta^2\text{H}$ ,  $\delta^{18}\text{O}$ , and altitude in waters.

extremely evaporated environment (Bowen et al., 2018; Craig, 1961). Furthermore, the lower slope values of  $\delta^2\text{H}$ - $\delta^{18}\text{O}$  line with strong evaporation have also been reported in southwest Montana by Gammons et al. (2006) and central Arctic of Canada by Gibson and Edwards (2002). Therefore, it can be inferred that the lower slope of the water line in rivers of the Chaiqu watershed may be related to the process of strong evaporation (Bowen et al., 2018). Furthermore, the slope of  $\delta^2\text{H}$ - $\delta^{18}\text{O}$  line may decrease due to the massive exchanges between liquids and solids in melt-freezing processes of the river water under low temperatures in winter (Shi et al., 2021b; Zhou et al., 2007). The highest values of  $\delta^2\text{H}$  and  $\delta^{18}\text{O}$  were found in CQ-2 (grass water with limited flow), which experienced repeated melt-freeze processes. The samples located at the lower reach of CQ-1 in the tributary have higher values of  $\delta^2\text{H}$  and  $\delta^{18}\text{O}$ , which may inherit characteristics from the grass water.

#### 4.2.2. Deuterium excess (*d*-excess)

To further analyze the hydrological process, the *d*-excess values were calculated in the study area. Most *d*-excess values were lower than 10% and higher *d*-excess values were found in high-altitude sites (Fig. 6b). The values of *d*-excess close to 10% indicate that the water is completely derived from precipitation (Ren et al., 2017). The higher values (>10%) of *d*-excess are generally caused by low humidity while lower *d*-excess values occur with abundant precipitation (Yan et al., 2021). It possibly indicated that the humidity was at a relatively high level in this high-altitude area. Most values of *d*-excess were lower than 10%, suggesting that the dominant factor in riverine isotopic compositions may be the regional hydrological cycle or other recharge contribution rather than the precipitation of the Chaiqu watershed. Woo (2012) suggested that rivers in the alpine regions were maintained in the runoff by active groundwater recharge during the dry season (especially in the freezing or early thawing period). The  $^{18}\text{O}$  in river water may increase during the interaction between water and rocks, while  $^2\text{H}$  is usually unaffected because of its low contents in rock minerals, resulting in the *d*-excess values decreasing (Yan et al., 2021). Based on the published data from the China Geological Survey (<https://doi.org/10.35080/data.C.2021.P23>), the freshwater-dominated super-permafrost water is wildly distributed in the study area with weak water storage properties. It implies that the groundwater is renewing rapidly with a weak water-rock reaction (Pan et al., 2022). However, *d*-excess values greater than 10% were also found in the upper reaches (CQ-1, CQ-4, CQ-5, CQ-6, and CQ-8) in the Chaiqu watershed except for grass water (CQ-2), suggesting that the contribution of groundwater had limited influence on  $\delta^2\text{H}$  and  $\delta^{18}\text{O}$  compositions. Other hydrological processes that occurred in river water after precipitation possibly govern the isotopic composition in the Chaiqu watershed.

Previous studies reported that the extent of increasing precipitation may not outweigh the effect of evaporation on riverine composition during the dry season, particularly in the alpine region (Sang et al., 2016; Zhou et al., 2007). Generally, the altitude is negative to the  $\delta^{18}\text{O}$  values in homogeneous moisture sources of river water and precipitation (Wu et al., 2019). The altitude had a positive correlation with *d*-excess values while a weakly negative correlation with  $\delta^{18}\text{O}$  values ( $R^2 = 0.163, p > 0.05$ ) in the Chaiqu watershed (Fig. 6b). Evaporation can enrich the heavier oxygen isotopes in the river water, which has been reported in several rivers and lakes in the TP (Jiao et al., 2015; Wang et al., 2022). The stronger evaporation with the flow may induce the  $^{18}\text{O}$  enrichment in river water. Generally, the sun-cloud evaporation will become progressively weaker with the altitude increasing (Craig, 1961). The river water was mainly derived from precipitation in the study area. Therefore, non-equilibrium fractionation of water molecules during evaporation may be the governing factor of riverine isotope composition in the study area.

#### 4.3. Environmental implication of hydrochemistry in alpine watersheds

The rivers in the TP are sensitive to environmental disturbances and

climate change due to ecological fragility (Tang et al., 2021). Compared with the rivers influenced by complex lithology at large scales in the TP, rivers in small watersheds can better reflect the factors controlling regional material transportation and the water cycle (Jiang et al., 2021). In contrast with previous study that the headwaters of the YTR are primarily influenced by groundwater contribution (Ren et al., 2016), it is more probable that alpine rivers receive more water supply from precipitation in this region. In general, rivers originating from precipitation will exhibit inherited hydrochemical characteristics (Sun et al., 2018). However, the isotopic compositions of alpine river waters may be not controlled by the intense evaporation process, but by precipitation or groundwater. The obvious variations of riverine ions within the Chaiqu watershed also respond to the heterogeneity within a limited catchment scale. The lower reaches of alpine rivers frequently represent the primary water source for residential towns. The downstream of the studied rivers also flow through a residential area (Laozhongba town). Generally, the ecosystem and water quality of the whole catchment are possibly affected by the headwater directly which causes environmental effects on surrounding areas. Therefore, the studies of alpine rivers on the TP to explore regional environmental change and responses to climate will help us to conduct the environmental assessments of the source rivers in alpine regions. Isotopic monitoring of rivers may help to subdivide the controlling factors of the eco-environment in alpine regions and optimize the water source management for the supplied residential areas.

## 5. Conclusions

This study comprehensively analyzed hydrogeochemical characteristics with major ions,  $\delta^2\text{H}$ , and  $\delta^{18}\text{O}$  in rivers from an alpine watershed located in the upper reaches of the YTR. The riverine fluxes of the Chaiqu watershed were of  $\text{HCO}_3\text{-Ca-Mg}$  type (58.82%) and  $\text{SO}_4\text{-Cl-Ca-Mg}$  type (41.18%), which was dominated by the weathering of carbonate and silicate. The primary contributor of  $\text{Cl}^-$  was halite dissolution, while the additional  $\text{Na}^+$  was contributed by silicate weathering. Dissolved  $\text{SO}_4^{2-}$  was more possibly derived from the oxidation of sulfides, and played a significant role in weathering processes and river solute origin. Based on the analyses of  $\delta^2\text{H}$  and  $\delta^{18}\text{O}$ , the river water originated mostly from direct precipitation with less contribution from groundwater in the upper reach. The enrichment of  $^{18}\text{O}$  was subject to strong evaporation rather than the influence of groundwater. The influence on riverine components is amplified by evapotranspiration without the glacial meltwater inputs, especially for the hydrogen and oxygen isotopic compositions. Clarifying hydrochemical characteristics and isotopic compositions in the alpine river can be useful to determine the mechanisms of hydrological cycle. The eco-fragility and harsh environmental conditions of the alpine watershed in the TP, make the recharge sources and material cycles sensitive to environmental changes (i.e., global warming). Consequently, hydrochemical monitoring is necessary to provide reliable datasets and scientific bases for water resource management and protection, as well as ecological conservation efforts in Tibetan alpine river basins in the background of global changes.

## Credit author statement

**Ruiyin Han:** Conceptualization, Data curation, Writing—original draft preparation, Writing—review and editing, **Wenjing Liu:** Methodology, Investigation, Data curation, Resources, Funding acquisition, **Jiangyi Zhang:** Investigation, Data curation, **Tong Zhao:** Sampling, Investigation, Data curation, **Huiguo Sun:** Sampling, Investigation, Data curation, Funding acquisition, **Zhifang Xu:** Conceptualization, Methodology, Investigation, Resources, Writing—original draft preparation, Writing—review and editing, Supervision, Funding acquisition.

## Declaration of competing interest

The authors declare that they have no known competing financial interests or personal relationships that could have appeared to influence the work reported in this paper.

## Data availability

Data will be made available on request.

## Acknowledgements

This research was financially supported by the “Strategic Priority Research Program” of the Chinese Academy of Sciences (grant No. XDB26000000), the National Key Research and Development Program of China (grant No. 2020YFA0607700), the National Natural Science Foundation of China (grant Nos. 41730857, 91747202, 42273050, 41877402), the Key Research Program of the Institute of Geology & Geophysics, CAS (grant No. IGGCAS-202204). Wenjing Liu acknowledges support from the Youth Innovation Promotion Association CAS (2019067).

## Appendix A. Supplementary data

Supplementary data to this article can be found online at <https://doi.org/10.1016/j.envres.2023.115981>.

**Table A.1**

The concentrations of dissolved major ions (mg/L) and isotopic compositions in the Chaiqu watershed.

Sample	T °C	pH	TDS mg/L	DO mg/L	Na <sup>+</sup>	K <sup>+</sup>	Mg <sup>2+</sup>	Ca <sup>2+</sup>	F <sup>-</sup>	Cl <sup>-</sup>	NO <sub>3</sub> <sup>-</sup>	SO <sub>4</sub> <sup>2-</sup>	HCO <sub>3</sub> <sup>-</sup>	δ <sup>18</sup> O ‰	δ <sup>2</sup> H ‰	d-excess ‰
CQ-1	1.70	6.8	90	2.50	8.82	0.69	13.64	54.57	0.12	7.05	2.98	161.86	63.90	-19.5	-143.2	13.2
CQ-2		7.0		2.20	4.26	0.97	4.48	16.41	0.77	3.52	2.00	6.28	74.75	-15.6	-126.3	-1.4
CQ-3	1.70	8.2	262	2.40	4.34	0.99	18.42	58.39	0.16	2.58	1.99	95.25	137.96	-19.1	-143.1	9.9
CQ-4	6.70	8.0	231	2.80	66.30	2.72	8.08	59.43	0.32	42.65	2.25	175.19	151.76	-19.5	-145.1	11.2
CQ-5	0.40	8.3	306	2.30	1.73	0.73	13.24	56.63	0.17	2.36	0.62	98.07	98.02	-19.5	-144.9	11.3
CQ-6	7.50	8.5	266	2.40	60.97	2.42	8.57	49.86	0.25	31.69	2.31	153.34	149.58	-19.2	-143.6	10.0
CQ-7	10.00	8.4	245	2.30	3.46	0.65	28.63	96.41	0.14	2.72	1.99	260.99	153.37	-18.1	-141.0	3.6
CQ-8	6.50	8.2	91	2.30	4.03	0.50	9.85	73.59	1.02	4.46	2.29	149.38	61.72	-18.9	-140.8	10.5
CQ-9	9.50	8.1	141	2.50	6.87	1.13	13.31	75.37	0.18	1.56	0.98	144.88	156.11	-18.4	-139.0	8.2
CQ-10	17.20	8.7	125	2.20	4.42	0.70	4.25	44.75	0.20	1.71	1.31	17.63	139.41	-18.3	-140.2	6.4
CQ-11	10.80	8.2	141	3.20	6.16	0.69	6.45	45.87	0.21	1.79	1.68	33.33	128.99	-18.1	-137.9	7.0
CQ-12	10.60	8.0	142	2.10	17.33	1.43	7.22	42.90	0.21	11.46	2.27	34.16	162.06	-17.6	-135.5	5.0
CQ-13	11.50	8.5	173	2.20	9.81	1.09	4.48	49.74	0.54	8.47	2.39	38.30	143.45	-18.9	-144.1	6.9
CQ-14	12.10	7.1	154	2.50	14.10	1.67	4.99	46.98	0.47	13.12	2.36	38.02	155.84	-18.8	-143.7	6.5
CQ-15	11.60	7.7	147	3.20	11.33	2.06	1.81	48.97	0.28	15.24	2.60	16.98	157.24	-19.0	-145.2	6.5
CQ-16	8.10	7.7	146	1.70	11.33	2.10	6.86	45.17	0.26	14.87	2.47	14.41	177.90	-18.9	-145.3	5.9
CQ-17	11.80	8.1	172	1.80	10.26	2.03	6.17	45.26	0.26	15.11	2.51	15.34	176.34	-18.8	-144.5	5.8
CQ-18	12.70	8.6	142	3.60	9.47	1.38	4.46	32.12	0.28	14.86	2.34	21.60	98.85	-18.7	-142.3	7.2

## References

- Bai, J.K., Li, C.L., Kang, S.C., Chen, P.F., Wang, J.L., 2014. Chemical speciation and risk assessment of heavy metals in the middle part of Yarlung Zangbo surface sediments. *Environ. Sci.* 35, 3346–3351.
- Bowen, G.J., Putman, A., Brooks, J.R., Bowling, D.R., Oerter, E.J., Good, S.P., 2018. Inferring the source of evaporated waters using stable H and O isotopes. *Oecologia* 187, 1025–1039.
- Craig, H., 1961. Isotopic variations in meteoric waters. *Science* 133, 1702–1703.
- Dai, D., Gao, J., Steen-Larsen, H.C., Yao, T., Ma, Y., Zhu, M., Li, S., 2021. Continuous monitoring of the isotopic composition of surface water vapor at Lhasa, southern Tibetan Plateau. *Atmos. Res.* 264, 105827.
- Dansgaard, W., 1964. Stable isotopes in precipitation. *Tellus* 16, 436–468.
- Das, P., Mukherjee, A., Hussain, S.A., Jamal, M.S., Das, K., Shaw, A., Layek, M.K., Sengupta, P., 2020. Stable isotope dynamics of groundwater interactions with Ganges river. *Hydrol. Process.* 35, e14002.
- Gaillardet, J., Dupré, B., Louvat, P., Allégre, C.J., 1999. Global silicate weathering and CO<sub>2</sub> consumption rates deduced from the chemistry of large rivers. *Chem. Geol.* 159, 3–30.
- Gammons, C.H., Poulson, S.R., Pellicori, D.A., Reed, P.J., Roesler, A.J., Petrescu, E.M., 2006. The hydrogen and oxygen isotopic composition of precipitation, evaporated mine water, and river water in Montana, USA. *J. Hydrol.* 328, 319–330.
- Gao, J., Ma, P., Du, J., Huang, X., 2020. Spatial distribution of extreme precipitation in the Tibetan Plateau and effects of external forcing factors based on Generalized Pareto Distribution. *Water Supply* 21, 1253–1262.
- Gibson, J.J., Edwards, T.W.D., 2002. Regional water balance trends and evaporation-transpiration partitioning from a stable isotope survey of lakes in northern Canada. *Global Biogeochem. Cycles* 16, 10–11, 10–14.
- Halder, J., Terzer, S., Wassenaar, L.I., Araguás-Araguás, L.J., Aggarwal, P.K., 2015. The Global Network of Isotopes in Rivers (GNIR): integration of water isotopes in watershed observation and riverine research. *Hydrol. Earth Syst. Sci.* 19, 3419–3431.
- Han, G., Liu, C., 2004. Water geochemistry controlled by carbonate dissolution: a study of the river waters draining karst-dominated terrain, Guizhou Province, China. *Chem. Geol.* 204, 1–21.
- Han, R., Zhang, Q., Xu, Z., 2023. Tracing Fe cycle isotopically in soils based on different land uses: insight from a typical karst catchment, Southwest China. *Sci. Total Environ.* 856, 158929.
- Hren, M.T., Chamberlain, C.P., Hilley, G.E., Blisniuk, P.M., Bookhagen, B., 2007. Major ion chemistry of the Yarlung Tsangpo–Brahmaputra river: chemical weathering, erosion, and CO<sub>2</sub> consumption in the southern Tibetan plateau and eastern syntaxis of the Himalaya. *Geochem. Cosmochim. Acta* 71, 2907–2935.
- Huang, X., Sillanpää, M., Gjessing, E.T., Peräniemi, S., Vogt, R.D., 2011. Water quality in the southern Tibetan plateau: chemical evaluation of the Yarlung Tsangpo (brahmaputra). *River Res. Appl.* 27, 113–121.
- Huang, X., Sillanpää, M., Gjessing, E.T., Vogt, R.D., 2009. Water quality in the Tibetan Plateau: major ions and trace elements in the headwaters of four major Asian rivers. *Sci. Total Environ.* 407, 6242–6254.
- Jiang, H., Liu, W., Li, Y., Zhang, J., Xu, Z., 2022. Multiple isotopes reveal a hydrology dominated control on the nitrogen cycling in the nujiang river basin, the last undammed large River Basin on the Tibetan plateau. *Environ. Sci. Technol.* 56, 4610–4619.
- Jiang, H., Liu, W., Xu, Z., Zhou, X., Zheng, Z., Zhao, T., Zhou, L., Zhang, X., Xu, Y., Liu, T., 2018. Chemical weathering of small catchments on the Southeastern Tibetan Plateau I: water sources, solute sources and weathering rates. *Chem. Geol.* 500, 159–174.
- Jiang, H., Zhang, Q., Liu, W., Zhang, J., Zhao, T., Xu, Z., 2021. Climatic and anthropogenic driving forces of the nitrogen cycling in a subtropical river basin. *Environ. Res.* 194, 110721.
- Jiang, L., Yao, Z., Wang, R., Liu, Z., Wang, L., Wu, S., 2015. Hydrochemistry of the middle and upper reaches of the Yarlung Tsangpo River system: weathering processes and CO<sub>2</sub> consumption. *Environ. Earth Sci.* 74, 2369–2379.
- Jiao, J.J., Zhang, X., Liu, Y., Kuang, X., 2015. Increased water storage in the qaidam basin, the north Tibet Plateau from GRACE gravity data. *PLoS One* 10.

- Li, P., Zhang, Y., Yang, N., Jing, L., Yu, P., 2016. Major ion chemistry and quality assessment of groundwater in and around a mountainous tourist town of China. *Exposure Health* 8, 239–252.
- Li, X., Han, G., Liu, M., Liu, J., Zhang, Q., Qu, R., 2022. Potassium and its isotope behaviour during chemical weathering in a tropical catchment affected by evaporite dissolution. *Geochim. Cosmochim. Acta* 316, 105–121.
- Li, Y., Liu, J., Gao, Z., Wang, M., Yu, L., 2020. Major ion chemistry and water quality assessment of groundwater in the Shigaze urban area, Qinghai-Tibetan Plateau, China. *Water Supply* 20, 335–347.
- Li, Z., Liu, J., Zhao, Y., Zhang, Y., Hu, Q., Liu, Y., Guo, H., 2021. Plateau river research: spatial-temporal variations of  $\delta^{18}\text{O}$  and  $\delta\text{d}$  in the water of the Yarlung Tsangpo River and their controlling factors. *Ecotoxicol. Environ. Saf.* 208, 111678.
- Liu, J., Han, G., 2020. Major ions and  $\delta^{34}\text{S}_{\text{SO}_4}$  in Jialongjiang River water: investigating the relationships between natural chemical weathering and human perturbations. *Sci. Total Environ.* 724, 138208.
- Liu, J., Song, X., Yuan, G., Sun, X., Yang, L., 2014. Stable isotopic compositions of precipitation in China. *Tellus B* 66, 22567.
- Liu, W., Jiang, H., Guo, X., Li, Y., Xu, Z., 2022a. Time-series monitoring of river hydrochemistry and multiple isotope signals in the Yarlung Tsangpo River reveals a hydrological domination of fluvial nitrate fluxes in the Tibetan Plateau. *Water Res.* 225, 119098.
- Liu, W., Jiang, H., Zhang, J., Xu, Z., 2022b. Driving forces of nitrogen cycling and the climate feedback loops in the Yarlung Tsangpo River Basin, the highest-altitude large river basin in the world. *J. Hydrol.* 610, 127974.
- Liu, W., Xu, Z., Jiang, H., Zhou, X., Zhao, T., Li, Y., 2023. Lithological and glacial controls on sulfide weathering and the associated  $\text{CO}_2$  budgets in the Tibetan Plateau: new constraints from small catchments. *Geochim. Cosmochim. Acta* 343, 341–352.
- Liu, Z., Tian, L., Yao, T., Gong, T., Yin, C., Yu, W., 2007. Temporal and spatial variations of  $\delta^{18}\text{O}$  in precipitation of the Yarlung zangbo river basin. *J. Geogr. Sci.* 17, 317–326.
- Marghade, D., Malpe, D.B., Zade, A.B., 2012. Major ion chemistry of shallow groundwater of a fast growing city of Central India. *Environ. Monit. Assess.* 184, 2405–2418.
- Mokarram, M., Pourghasemi, H.R., Huang, K., Zhang, H., 2022. Investigation of water quality and its spatial distribution in the Kor River basin, Fars province, Iran. *Environ. Res.* 204, 112294.
- Ogwueleka, T.C., 2014. Assessment of the water quality and identification of pollution sources of Kaduna River in Niger State (Nigeria) using exploratory data analysis. *Water Environ. J.* 28, 31–37.
- Pan, Y., Sun, Z., Pan, Z., Zhang, S., Li, X., Ma, R., 2022. Influence of permafrost and hydrogeology on seasonal and spatial variations in water chemistry of an alpine river in the northeastern Qinghai-Tibet Plateau, China. *Sci. Total Environ.* 834, 155227.
- Pant, R.R., Zhang, F., Rehman, F.U., Wang, G., Ye, M., Zeng, C., Tang, H., 2018. Spatiotemporal variations of hydrogeochemistry and its controlling factors in the gandaki river basin, central Himalaya Nepal. *Sci. Total Environ.* 622–623, 770–782.
- Qu, B., Sillanpää, M., Zhang, Y., Guo, J., Wahed, M.S.M.A., Kang, S., 2015. Water chemistry of the headwaters of the Yangtze river. *Environ. Earth Sci.* 74, 6443–6458.
- Ren, W., Yao, T., Xie, S., 2016. Water stable isotopes in the Yarlungzangbo headwater region and its vicinity of the southwestern Tibetan Plateau. *Tellus B* 68, 30397.
- Ren, W., Yao, T., Xie, S., He, Y., 2017. Controls on the stable isotopes in precipitation and surface waters across the southeastern Tibetan Plateau. *J. Hydrol.* 545, 276–287.
- Sang, Y., Singh, V.P., Gong, T., Xu, K., Sun, F., Liu, C., Liu, W., Chen, R., 2016. Precipitation variability and response to changing climatic condition in the Yarlung Tsangpo River basin, China. *J. Geophys. Res. Atmos.* 121, 8820–8831.
- Shi, D., Tan, H., Chen, X., Rao, W., Basang, R., 2021a. Uncovering the mechanisms of seasonal river–groundwater circulation using isotopes and water chemistry in the middle reaches of the Yarlungzangbo River, Tibet. *J. Hydrol.* 603, 127010.
- Shi, D., Tan, H., Chen, X., Rao, W., Issombo, H.E., Basang, R., 2021b. Temporal and spatial variations of runoff composition revealed by isotopic signals in Nianchu River catchment, Tibet. *J. Hydrol.* 37, 1–12.
- Sun, C., Shen, Y., Chen, Y., Chen, W., Liu, W., Zhang, Y., 2018. Quantitative evaluation of the rainfall influence on streamflow in an inland mountainous river basin within Central Asia. *Hydrol. Sci. J.* 63, 17–30.
- Tan, H., Chen, X., Shi, D., Rao, W., Liu, J., Liu, J., Eastoe, C.J., Wang, J., 2021. Base flow in the Yarlungzangbo River, Tibet, maintained by the isotopically-depleted precipitation and groundwater discharge. *Sci. Total Environ.* 759, 143510.
- Tan, H., Zhang, Y., Zhang, W., Kong, N., Zhang, Q., Huang, J., 2014. Understanding the circulation of geothermal waters in the Tibetan Plateau using oxygen and hydrogen stable isotopes. *Appl. Geochem.* 51, 23–32.
- Tang, P., Xu, B., Tian, D., Ren, J., Li, Z., 2021. Temporal and spatial variations of meteorological elements and reference crop evapotranspiration in Alpine regions of Tibet, China. *Environ. Sci. Pollut. Control Ser.* 28, 36076–36091.
- Tian, L., Yu, W., Schuster, P.F., Wen, R., Cai, Z., Wang, D., Shao, L., Cui, J., Guo, X., 2020. Control of seasonal water vapor isotope variations at Lhasa, southern Tibetan Plateau. *J. Hydrol.* 580, 124237.
- Wang, F., Zhao, Y., Chen, X., Zhao, H., 2019. Hydrochemistry and its controlling factors of rivers in the source region of the nujiang river on the Tibetan plateau. *Water* 11, 2166.
- Wang, L., Liu, W., Xu, Z., Zhang, J., 2022. Water sources and recharge mechanisms of the Yarlung Zangbo River in the Tibetan Plateau: constraints from hydrogen and oxygen stable isotopes. *J. Hydrol.* 614, 128585.
- Wang, R., Yao, Z., Liu, Z., 2020. Change of contributions from different natural processes to the ionic budget in the Yarlung Tsangpo River. *Water* 12.
- Woo, M.-k., 2012. Permafrost Hydrology. Springer Berlin. Springer-Verlag Berlin Heidelberg, Heidelberg.
- Wu, H., Wu, J., Song, F., Abuduwalli, J., Saparov, A.S., Chen, X., Shen, B., 2019. Spatial distribution and controlling factors of surface water stable isotope values ( $\delta^{18}\text{O}$  and  $\delta^{2\text{H}}$ ) across Kazakhstan, Central Asia. *Sci. Total Environ.* 678, 53–61.
- Wu, W., Yang, J., Xu, S., Yin, H., 2008. Geochemistry of the headwaters of the Yangtze river, tongtian Hu and jinsha Jiang: silicate weathering and  $\text{CO}_2$  consumption. *Appl. Geochem.* 23, 3712–3727.
- Xiao, J., Lv, G., Chai, N., Hu, J., Jin, Z., 2022. Hydrochemistry and source apportionment of boron, sulfate, and nitrate in the Fen River, a typical loess covered area in the eastern Chinese Loess Plateau. *Environ. Res.* 206, 112570.
- Xuan, W., Xu, Y., Fu, Q., Booij, M.J., Zhang, X., Pan, S., 2021. Hydrological responses to climate change in Yarlung zangbo river basin, southwest China. *J. Hydrol.* 597, 125761.
- Yan, Y., Zhang, J., Zhang, W., Zhang, G., Guo, J., Zhang, D., Wu, J., Zhao, Z., 2021. Spatiotemporal variation of hydrogen and oxygen stable isotopes in the Yarlung Tsangpo River basin, southern Tibetan plateau. *Foront. Earth Sci.* 9, 757094.
- Yang, K., Han, G., 2020. Controls over hydrogen and oxygen isotopes of surface water and groundwater in the Mun River catchment, northeast Thailand: implications for the water cycle. *Hydrogeol. J.* 28, 1021–1036.
- Yang, Q., Li, Z., Ma, H., Wang, L., Martin, J.D., 2016. Identification of the hydrogeochemical processes and assessment of groundwater quality using classic integrated geochemical methods in the Southeastern part of Ordos basin, China. *Environ. Pollut.* 218, 879–888.
- Zeng, J., Han, G., Zhang, S., Liang, B., Qu, R., Liu, M., Liu, J., 2022. Potentially toxic elements in cascade dams-influenced river originated from Tibetan Plateau. *Environ. Res.* 208, 112716.
- Zeng, J., Han, G., Zhang, S., Qu, R., 2023. Nitrate dynamics and source identification of rainwater in Beijing during rainy season: insight from dual isotopes and Bayesian model. *Sci. Total Environ.* 856, 159234.
- Zhang, F., Zeng, C., Zhang, Q., Yao, T., 2022a. Securing water quality of the asian water tower. *Nat. Rev. Earth Environ.* 3, 611–612.
- Zhang, T., Cai, W., Li, Y., Geng, T., Zhang, Z., Lv, Y., Zhao, M., Liu, J., 2018. Ion chemistry of groundwater and the possible controls within Lhasa river basin, SW Tibetan plateau. *Arabian J. Geosci.* 11, 510.
- Zhang, X., Xu, Z., Liu, W., Moon, S., Zhao, T., Zhou, X., Zhang, J., Wu, Y., Jiang, H., Zhou, L., 2019. Hydro-Geochemical and Sr isotope characteristics of the yalong river basin, eastern Tibetan plateau: implications for chemical weathering and controlling factors. *G-cubed* 20, 1221–1239.
- Zhang, Z., Guo, Y., Wu, J., Su, F., 2022b. Surface water quality and health risk assessment in taizhou city, zhejiang province (China). *Exposure Health* 14, 1–16.
- Zhao, T., Liu, W., Xu, Z., Sun, H., Zhou, X., Zhou, L., Zhang, J., Zhang, X., Jiang, H., Liu, T., 2019. The influence of carbonate precipitation on riverine magnesium isotope signals: new constrains from Jinsha River Basin, Southeast Tibetan Plateau. *Geochim. Cosmochim. Acta* 248, 172–184.
- Zhou, S., Nakawo, M., Hashimoto, S., Sakai, A., 2007. The effect of refreezing on the isotopic composition of melting snowpack. *Hydrol. Process.* 22, 873–882.
- Zhou, M., Kuang, X., Feng, Y., Hao, Y., He, Q., Zhou, H., Chen, J., Zou, Y., Zheng, C., 2021. Hydrochemistry of the Lhasa river, Tibetan plateau: spatiotemporal variations of major ions compositions and controlling factors using multivariate statistical approaches. *Water* 13, 3660.